A BIOLOGICAL VISION INSPIRED FRAMEWORK FOR IMAGE ENHANCEMENT IN POOR VISIBILITY CONDITIONS USING ANISOTROPIC DIFFUSION FILTER

PROJECT REPORT

Submitted by

REHNA CHERIAN KATTAKAYAM

REG NO : TKM20CSCE11

In partial fulfillment for the award of the degree of

MASTER OF TECHNOLOGY
IN
COMPUTER SCIENCE AND ENGINEERING

Under the guidance of
Dr. Dimple A. Shahjahan

Thangal Kunju Musaliar College of Engineering
Kerala

SEPTEMBER 2022

Thangal Kunju Musaliar College of Engineering
Dept. of Computer Science & Engineering

C E R T I F I C A T E

This is to certify that this report titled ***A Biological Vision Inspired Framework for Image Enhancement in Poor Visibility Conditions Using Anisotropic Diffusion Filter*** is a bonafide record of the **Project** presented by **REHNA CHERIAN KATTAKAYAM (TKM20CSCE11)**, under our guidance and supervision, in partial fulfillment of the requirements for the award of the degree, **M.Tech in Computer Science & Engineering** in **APJ Abdul Kalam Technological University** .

Coordinator

Dr. Ansamma John
Professor
Dept. of CSE
TKMCE

Supervisor & Head of the Department

Dr. Dimple A. Shahjahan
Associate Professor
Dept. of CSE
TKMCE

ACKNOWLEDGEMENT

A successful project is a fruitful culmination of efforts by many people, some directly involved and some others indirectly, by providing support and encouragement. Firstly, I would like to thank the Almighty for giving me the wisdom and grace for making my project a memorable one. I thank him for steering me to the shore of fulfillment under his protective wings.

I express my sincere gratitude to **Dr. T A Shahul Hameed** , Principal of T.K.M College of Engineering for giving me an opportunity to present my project. I would like to thank **Dr. Dimple A. Shahjahan**, Associate Professor and Head of the Department, CSE, TKMCE, for her constant support and encouragement throughout the project work.

With a profound sense of gratitude, I would like to express my heartfelt thanks to my guide **Dr. Dimple A. Shahajahan**, Associate Professor, CSE, TKMCE for her expert guidance, cooperation and immense encouragement. I also extend my thanks to all faculty members and staff of the Department of Computer Science and Engineering, TKMCE, who has encouraged me throughout this work.

I also express my thanks to my loving parents, sisters and friends, for their support and encouragement in the successful completion of this project work.

Rehna Cherian Kattakayam

Abstract

Image enhancement with edge retention in the presence of outliers and artefacts is a daunting task in the field of image processing and computer vision. Inspired by the information processing mechanism in the human retina, an effective two-pathway image enhancement framework that incorporates anisotropic diffusion smoothing filter is developed, which aids in the low dynamic range image enhancement. The input image is decomposed into two layers using TV-L1 denoising method into base layer and detail layer and are sent into two channels, namely, structure pathway and detail pathway, which processes the low and high frequency information of the input visual images. In the structure-pathway, a normalization model incorporating the local and global visual adaptation terms is used, which manifested better performance in the case of the visual scenes with fluctuating illumination conditions. Furthermore, the detail enhancement and noise suppression are achieved in the detail-pathway based on local energy weighting. The outputs of two channels are unified and is eventually subjected to Perona Malik diffusion filter to achieve the low-light and night-time image enhancement. Experimental results on LDR image dataset called PKUnight corroborated that the proposed bioinspired image enhancement framework contributes well to the image enhancement tasks efficiently and outperform the related state-of-the-art techniques in terms of standard image quality evaluation metrics.

Contents

List of Figures

List of Tables

Chapter 1

Introduction

The nighttime image enhancement plays a pivotal role in many real life applications. In night time and twilight scenes, due to the low brightness and low contrast, the features of images such as color, corners, ridges and edges become vague, which resulted in deplored performance of current image processing methods. Effectual and robust nighttime image enhancement techniques should improve the contrast and the brightness of nighttime image, and also suppress noise and preserve details of such images. However, contemporary nighttime image enhancement methods cannot fulfill all the requirements of users.

Some state-of-the-art image enhancement techniques are able to extract features from the original images captured in daytime. However, in nighttime images, the brightness and the contrast between background and object are so low that some high frequency information of the images become obscure. Hence, there is a need to enhance the brightness, contrast and high frequency details of the lowlight and nighttime images.

Inspired by the retinal information processing mechanisms of the human visual system, an efficient nighttime image enhancement framework is developed that models a unified two pathway model incorporating Perona – Malik diffusion filter. Using such denoising filters can improve the performance of current detection methods. In this work, the denoising approach called anisotropic diffusion filter, also called Perona–Malik model is used, which aims at reducing the noise content of the image without removing high frequency components such as edges, lines or other details that are salient for the elucidation of an image.

The prime focus of traditional image enhancement methods is on adjusting

the histogram of input images to demonstrate more visual details of an image. Various types of histogram equalization (HE) such as adaptive histogram equalization (AHE) [12], bi-histogram equalization (BHE) [13], multipeak histogram equalisation(MPHE), multipurpose beta optimised bi-histogram equalisation and contrast limited adaptive histogram equalization (CLAHE) [14]) aim at adjusting the distribution of histogram by using different regularization terms. Moreover, variational and contextual contrast enhancement techniques utilize contextual information for nonlinear data mapping of visual inputs [15]. A contrast enhancement method was developed based on the layered difference representation of two-dimensional (2D) histogram.

A well known theory, called Retinex theory, assumes that an image can be decomposed into two main components, i.e., reflectance and illumination [17].Different versions of Retinex theory such as single-scale Retinex (SSR) [18], multi-scale Retinex (MSR) [19], multiscale Retinex with color restoration etc. have been developed. A weighted variational model is one of the most recent development for simultaneous reflectance and illumination estimation (SRIE). This model can preserve more details by suppressing the noises to a certain extent [21].

The common goal of the aforementioned methods is the detail preservation or even detail enhancement of the visual images.These methods can achieve fine performance for dynamic range compression of input visual images. The biological visual system is an efficient system that can improve the quality of the visual images. Most of the studies have proved that the divisive normalization plays a crucial role in the visual adaptation process [45]. The divisive normalization serves as a canonical neural computation mechanism and helps in the visual light adaptation [45], [48]. From the perspective of human visual system, the retina is considered as the fundamental unit of visual information processing system. The basic function of retina is to sense the incident light and sent them to brain as electrical signals [9], [46]. The human retina has the ability of adjusting the wide range of intensity levels of scenes to the operating range of the human nervous system. The contribution of divisive normalization models have shown superior performance in many image enhancement tasks [49].

Parallel information processing channels in the retina play vital roles in human visual processing [51]. The human retina consists of two types of cells, namely, Midget cells and Parasol cells. The input visual signals are processed in the retina with two types of cells, i.e., Midget cells and Parasol cells [51], [52].Midget cells are a type of retinal ganglion cell that helps in the processing of high frequency information such as details, edges, corners and ridges. Parasol cells are also a type of ganglion cells found in primates, which helps in the processing of low frequency information, for example, long unchanging spaces and structure of an image.[52] The main difference between Midget cells and Parasol cells is the midget ganglion cells have smaller receptive fields than parasol ganglion cells. Moreover, most of the motion related information are processed in the parasol ganglion cells. In the biological visual system, Magnocellular pathway (M-pathway) and Parvocellular pathway (P-pathway) are two main channels in the neuronal machinery. In the field of neuroscience and cognitive psychology, the two-pathway strategy and visual adaptation with Perona Malik diffusion filter have demonstrated superior performance compared to the state-of-the-art technologies.

With the advent of modern digital cameras and its increasing usage, the haze removal of low light and night time images have gained significant attention. Image enhancement has got wide applications in numerous scientific fields such as agronomy, surveillance, astronomy, medical sciences etc.. Image decomposition has been used extensively in image processing [56],computer graphics and computational photography, such as image smoothing [57], image abstraction and detail enhancement.

In this report, the focus is primarily on low dynamic range image enhancement. The common goal of this task is to enhance the details for the better elucidation of the visual images. In summary, we have developed a novel and robust bio-inspired two pathway model integrated with anisotropic diffusion filter for low dynamic range image enhancement. Inspired by the divisive normalisation models in the image processing tasks, a normalisation model was used to incorporate the local and global visual adaptation terms. The use of anisotropic diffusion filter have shown fine performance compared to the existing methods in terms of numerous quality evaluation metrics.

The remainder of this report is constructed as follows: Chapter 2 recalls some related works used as reference for completing this study. Chapter 3 details the process of generating the trimap of a fundus image automatically, and the proposed hierarchical image matting model. Chapter 4 introduces the public available datasets and the experimental results. The conclusion is provided in Chapter 5.

Chapter 2

Related Works

Image enhancement has become an important research field in recent years. Here, a brief review of the most relevant and best-performing approaches of various studies and the methods are discussed.

2.1 Nonlinear total variation based noise removal algorithms

Rudin et al.[1] presented a constrained optimization style of numerical algorithm for removing noise from images. The overall variation of the image is minimized by taking the statistics of the noise. The constraints are imposed using Lanrange multipliers. The answer is obtained using the gradient projection method. This amounts to solving a time dependent partial equation which is determined by the predefined constraints. As the value of t tends to infinity, the answer converges to a gradual state, which is the desired denoised image. The numerical algorithm is straightforward and comparatively fast. The results appear to be state-of-the-art for very noisy images. The tactic is noninvasive, yielding sharp edges within the image. The technique might be interpreted as a primary step of moving each level set of the image normal to itself with velocity capable the curvature of the amount set divided by the magnitude of the gradient of the image, and a second step which projects the image back onto the constraint set.

2.2 Structure-Texture Image Decomposition—Modeling, Algorithms, and Parameter Selection

Aujol et al.[2] explored the various aspects of the image decomposition problem using modern variational techniques. This work aims at splitting an

explicit image I into two components u and v, where u holds the geometrical information and v holds the textural information. The most focus of this work is to check different energy terms and functional spaces that suit the various styles of textures. The modeling uses the total-variation energy for extracting the structural part and one among four of the subsequent norms for the textural part: L^2, G, L^1 and a replacement tunable norm, suggested here for the primary time, supported Gabor functions. other than the broad perspective and our suggestions when each model should be used, the work contains three specific novelties, the correlation graph between u and v is an efficient tool to pick out the splitting parameter, a new fast algorithm to unravel the TV-L1 minimization problem is developed, and the idea and style tools for the TV-Gabor model is introduced.

2.3 Fast Noise Variance Estimation

John Immerkaer [3] developed a quick and straightforward method for estimating the variance of additive zero mean Gaussian noise in a picture. The strategy can also be used to provide a local estimate of the noise variance within the situation in which the noise variance varies across the image. It requires only the employment of a 3×3 mask followed by a summation over the image or a neighborhood neighborhood. A total of 14 integer operations per pixel is critical. The tactic performs well for an outsized range of noise variance values. In highly textured images or regions, though, the noise estimator perceives thin lines as noise.

2.4 Nighttime image enhancement based on image decomposition

A nighttime image enhancement method based on image decomposition was proposed by Xuesong Jiang et al. [4]. A nighttime image taken in a low- or unevenly illuminated environment always has a loss of visibility and is full of unwanted noise and artefacts. The noise and artefact will also be exacerbated as we increase the brightness's amplitude. As a result, a technique to nighttime picture enhancement based on image decomposition is suggested. The input image is divided into two layers: the texture layer contains the

details, noise, and artefacts, while the structure layer holds the primary information of the input image. The structure layer is enhanced using a more effective retinex image enhancement technique. The mask-weighted least squares method is employed in the texture layer to preserve features and reduce noise and artefacts. In the end, these two elements are combined to produce the desired outcome. The results of the experiments show that the suggested method can enhance the perceptual quality of nighttime photos while suppressing noise and artefact without using too much reinforcement.

2.5 Model of retinal local adaptation for the tone mapping of color filter array images

Meylan et al. [5] presented a tone mapping algorithm that is derived from a model of retinal processing. This approach has two major improvements over existing methods. As with the human visual system, which applies a non-linearity to the chromatic responses acquired by the cone mosaic, tone mapping is first applied directly to the mosaic image captured by the sensor. This reduces the number of necessary operations by a factor 3. Also, a variation of the center/surround class of local tone mapping algorithms is introduced, which are known to increase the local contrast of images but tend to create artifacts. This method gives a good improvement in contrast while avoiding halos and maintaining good global appearance. Like traditional center/surround algorithms, this method uses a weighted average of surrounding pixel values. Instead of being used directly, the weighted average serves as a variable in the Naka–Rushton equation, which models the nonlinearity of photoreceptors. This algorithm provides pleasing results on various images with different scene content and dynamic range.

2.6 Divisive Normalization in Population Codes

Olsen et al.[6] have proved that a normalization occurs during olfactory processing in the Drosophila antennal lobe. Researchers have exploited the orderly anatomy of this circuit to independently manipulate feedforward and lateral input to second-order projection neurons (PNs). Lateral inhibition increases the level of feedforward input needed to drive PNs to saturation, and this normalization scales with the total activity of the olfactory recep-

tor neuron (ORN) population. Increasing total ORN activity also makes PN responses more transient. Strikingly, a model with just two variables (feed-forward and total ORN activity) accurately predicts PN odour responses. Finally, it is shown that the discrimination by a linear decoder is facilitated by two complementary transformations: the saturating transformation intrinsic to each processing channel boosts weak signals, while normalization helps equalize responses to different stimuli.

2.7 A non-local algorithm for image denoising

A. Buades, B. Coll and J.Morel[7] proposed a new measure, to evaluate and compare the performance of digital image denoising methods. Noise is computed and analyzed for a wide class of denoising algorithms, namely the local smoothing filters.Also, a new algorithm is proposed, the nonlocal means (NL-means), based on a nonlocal averaging of all pixels in the image. Extensive experiments are done for comparing the NL-means algorithm and the local smoothing filters.

2.8 Image Denoising by Sparse 3-D Transform-Domain Collaborative Filtering

Dabov et al.[8] proposed a unique image denoising strategy supported by an enhanced sparse representation in transform domain. The enhancement of the sparsity is achieved by grouping similar 2D image fragments into 3D data arrays which are also known as "groups". Collaborative Altering may be a special procedure developed to cope with these 3D groups. This can be realized using the three successive steps: 3D transformation of a bunch, shrinkage of the transform spectrum, and inverse 3D transformation. The result is a 3D estimate that consists of the jointly filtered grouped image blocks. By attenuating the noise, the collaborative filtering reveals even the best details shared by grouped blocks and, at the identical time, it preserves the essential unique features of each individual block. The filtered blocks are then returned to their original positions. Because these blocks are overlapping, for every pixel, many different estimates are obtained which need to be combined. Aggregation may be a particular averaging procedure which is exploited to require advantage of this redundancy. A big improvement is ob-

tained by a specially developed collaborative Wiener filtering. An algorithm supported this novel denoising strategy and its efficient implementation are presented fully detail; an extension to color-image denoising is additionally developed. The experimental results demonstrate that this computationally scalable algorithm achieves state-of-the-art denoising performance in terms of both peak signal-to-noise and subjective visual quality.

Chapter 3

Methodology

In this study, an image improvement architecture is suggested that was inspired by the parallel pathways in the primitive visual system. In this work, an image enhancement architecture based on two visual streams, i.e., structure-pathway and detail- pathway is developed, inspired by the parallel pathways in the early visual system. Figure 3.1 provides a summary of the conceptual design of the suggested model. The first step is to segregate and send the input visual image into these two parallel routes. In particular, the structure pathway transmits and processes low frequency information (such as brightness) and uses visual adaptation mechanisms to reduce the image luminance to a tolerable level. In the detail-pathway that transmits the high frequency information, noises are reduced while structural features are maintained (e.g., the details and noises). The brightness correction, noise suppression, and detail enhancement are accomplished by combining the outputs of the structure-pathway and detail-pathway. Finally, the resulting output is eventually subjected to an anisotropic diffusion filter to further denoise the image and to enhance the visual naturalness of an image.

3.1 Pathway Separation with Global Noise Estimation

Images taken in low light, especially at night, frequently have loud noises. During the processing of image enhancement, the sounds must be suppressed or eliminated in order to increase the visual quality of such images. In general, directly enhancing a scene's lighting also intensifies its noises, which will make noise removal or suppression more challenging. Since the visual pathways are distinct, the luminance can be adjusted in the structure-pathway and the noises have been modified (improved). In the detail-pathway, noise suppression is accomplished. Biologically, Li et al. [59] discovered that some cat LGN cells react poorly to the stimulus of widely spaced out dots, in com-

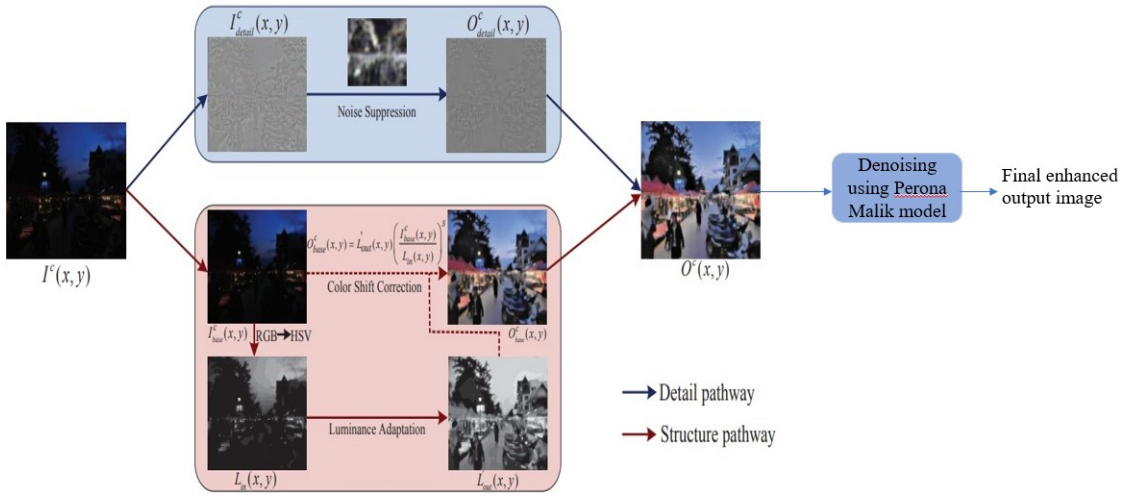

Figure 3.1: The framework of the proposed model inspired by the biological visual mechanisms.

parison to those of the densely spaced out dots (like the scattered dots are gathered into a line). From the perspective of engineering, denoising can be accomplished using image decomposition techniques. For instance, the noise reduction algorithm proposed by Rudin et al. is based on the TV model [57], which eliminates the noise layer to achieve denoising using image decomposition based on Total Variation. This work does not remove the detail layer that the TV-based system has broken down immediately, but use noise cancellation and attenuation to details in the detail layer preserving.

We use the total-variation (TV) energy based image decomposition algorithm [2] to divide the input image into two routes. Firstly, it is possible to think of the input image $I^c(x, y)$ as the superimposition of the two layers:

$$I^c(x,y) = I^c_{base}(x,y) + I^c_{detail}(x,y) \tag{3.1}$$

After that, the base layer is obtained by minimising the following objective function based on the TV regularisation presented in [2].

$$min_{I^c_{base}} \sum_{(x,y)} (I^c_{base}(x,y) - I^c(x,y))^2 + \lambda^c |\nabla I^c_{base}(x,y)| \tag{3.2}$$

This objective function has two terms. The first is a difference term tailored to the texture component, which helps to preserve the meaningful structure [57]. The second term is a regularisation term based on the total variation. It helps to reduce the amount of details in the image. The operator ∇ stands for the gradient operator, and the value of λ^{c} is set to be 2 times the global noise estimation (ϵ), that is, $\lambda^{\mathrm{c}} = 2\epsilon^{\mathrm{c}}$, $\mathrm{c} \in \{\mathrm{r}, \mathrm{g}, \mathrm{b}\}$. Setting $\lambda^{\mathrm{c}} = 2\epsilon^{\mathrm{c}}$ serves primarily to ensure that noises and a portion of high frequency details (such as fine edges) are separated into the detail layer. As a result, the detail-pathway can achieve noise suppression and detail enhancement without being disturbed by the low-frequency information.

It is possible to calculate the global noise estimation (ϵ^{c}) using [60].

$$\epsilon^{c} = \sqrt{\frac{\pi}{2}} \frac{1}{6(W-2)(H-2)} \sum_{(x,y)} |(I^{c} * N_{s})(x,y)| \tag{3.3}$$

$$N_{s} = \begin{bmatrix} 1 & -2 & 1 \\ -2 & 4 & -2 \\ 1 & -2 & 1 \end{bmatrix} \tag{3.4}$$

where $*$ stands for the convolution operator and $\mathrm{c} \in \{\mathrm{r}, \mathrm{g}, \mathrm{b}\}$. H and W stand for the height and width of the image (in pixels), respectively (I^{c}). The magnitude (size) of the high-frequency component, which is utilised to calculate the regularisation parameter in (3.2), can be roughly estimated using (3.4). The high-frequency component that will be transmitted into the detail-pathway can therefore be determined using the suggested method in an adaptive manner.

By figuring out (3.2), we can get the base layer, which contains the primary structure of the scene. The detail layer can therefore be easily obtained by subtracting base layer from the original image.

$$I^{c}_{detail}(x,y) = I^{c}(x,y) - I^{c}_{base}(x,y) \tag{3.5}$$

Several instances of image decomposition with global noise estimation are shown in Fig. 3.2. From Fig. 3.2, it is obvious that the base layer primarily contains the brightness information, whereas the detail layer contains the finer features and noise. As a result, the base layer information will be communicated in the structure-pathway, therefore changing the brightness in the structure-pathway will not exacerbate the noises already present in the detail-pathway. On the other hand, the noise suppression in the detail-pathway will be facilitated by the detail layer being isolated from the brightness, as explained below.

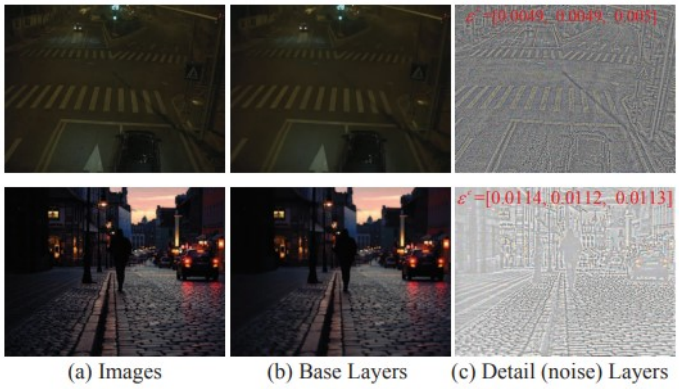

Figure 3.2: Examples of image decomposition with global noise estimation. The numbers listed in the detail maps are the global noise estimations for the R,G and B channels respectively.

Be aware that from the perspective of image processing, breaking down an image into different scales is a standard technology, especially in the fields of image enhancement. Structure-texture decomposition is one technique that has been frequently employed in image processing [2]. The structure-texture decomposition was explored in this work, but, from the perspective of the biological visual system. Additionally, we used global noise estimation for parameter tuning.

3.2 Luminance Adaptation in Structure Pathway

In this approach, the structure pathway allows for both brightness adjustment and visual adaptation. It is necessary to convert the base layer of the given image from RGB to HSV colour space to retrieve the luminance information, and then extract the luminance information from the V channel. With little quality loss, this colour conversion has been routinely employed for image improvement applications [21] - [23].

Some visual photoreceptor response models have been put forth in accordance with the well-known Naka-Rushton (NR) equation, which was created to fit the responsive curves for the rods and cones in the biological visual system [48], in order to adjust the luminance of the given image to a reasonable range. The traditional Naka-Rushton equation has the formula as given below,

$$R(x,y) = \frac{L(x,y)^n}{L(x,y)^n + \sigma^n} \tag{3.6}$$

It defines an S-shaped responsive curve. *L(x, y)* denotes the intensity of the visual input. The mean of the S-shape curve on the log input luminance axis is controlled by the global adaptation factor (a constant denoting the input light level) in Fig. 3.3(left). The scaling of the global contrast is influenced by the slope of the S shaped curve, which is controlled by n (Fig. 3.3(right)). As a result, it is possible to think of visual adaptation processing as the adjustment of σ and n in accordance with the input visual scenes or the local areas of the scenes.

A straightforward, yet effective method for visual adaptation is offered by the traditional NR equation in equation (3.6). This NR equation is, however, typically ineffective for adjusting to local visual inputs. A global adaptation level (σ), especially for nighttime pictures, cannot effectively capture the local aspects of the significantly variable illumination in various image regions. The neural responses in the fly olfactory system have recently been better described by a revised equation that includes a new local term [55]. It should be mentioned that a fly's vision differs significantly from a human's.

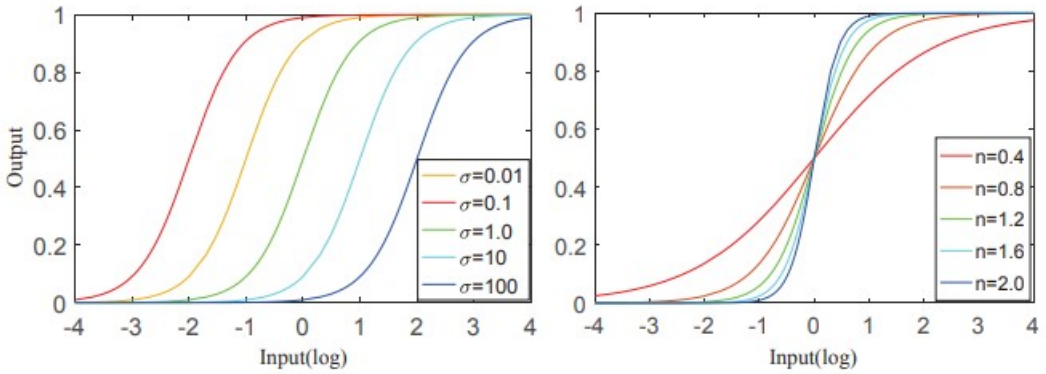

Figure 3.3: The responsive curves generated with Naka-Rushton. Left: the responsive curves when varying σ with fixed n ; Right: the responsive curves when varying n with fixed σ.

Normalization, however, may be a canonical neural computation in such a diversity of visual systems across numerous animals, according to some studies [45]. This motivates us to change the traditional NR equation in this study to merge the local and global visual adaptation in a weighted manner.Because the traditional Naka-Rushton equation is a global equation, we computationally altered the NR equation to include the spatial dependence in the luminous regulation [45].

$$L_{out}(x,y) = \frac{L_{in}(x,y)^n}{L_{in}(x,y)^n + \omega_l(x,y).\sigma_l(x,y)^n + \omega_g(x,y).(\sigma_g)^n} \tag{3.7}$$

$L_{in}(x,\ y)$ in (3.7) refers to the luminance channel of the base layer for the specified image. The local adaptation level (ω_{l}(x, y)), which varies with the local areas of the image, and the global adaptation level (σ_{g}), which is approximated from the entire image, are the two components that determine the visual adaptation level. This technique therefore evaluates the global and local adaptation terms for an input image first. According to the local brightness of the scene, $\omega_{\ g}(x,\ y)$ and $\omega_{\ l}(x,\ y)$ are the weights used to balance the contributions of the global and local adaption variables.The weights, global and local adaptation factors, and the modified luminance map ($L_{out}(x,\ y)$) are computed as follows.

First, let us define M_σ as the average pixel intensity and S_σ as the standard deviation for the luminance channel of the image. Calculating the global adaptability factor (σ_g) is as follows:

$$\sigma_g = \frac{M_g}{1 + \omega_s . S_g} \tag{3.8}$$

where ω_s is a variable that regulates how much the standard deviation contributes. We simply trimmed the pixels with values outside of the range of 0.5% 99.5% intensity level in order to prevent the unfavourable influence of the excessively bright or dark pixels on the mean and standard deviation estimations.

The global adaption factor denoted as (σ_g) in Equation (3.8), is dependent on the global mean (M_g) and standard deviation (S_g) of the luminance adjusted map. The outcome is that a darker scene generates a smaller σ_g, which leads to a higher brightness improvement, and vice versa. For certain situations with both significant dark and bright sections, or for images with a bimodal distribution of the histogram, the standard deviation term (S_g) is employed to correct the calculation of the global adaption factor.

When employing merely the global mean, an image with more bright pixels would produce a bigger global mean, which would be ineffective for the dark regions because it would overestimate the global adaption factor. However, because S_g is typically much smaller than 1.0, S_g has a minimal impact on the majority of scenes. Additionally, we may easily eliminate the standard deviation (S_g) term by setting s = 0 for particular situations.

The global adaption term can change the overall luminance of the input image, but it cannot improve some localised low-light areas, especially when the dark and bright areas are present in the same scene. Therefore, to further alter the local luminance of the scenes, we define the term "local intensity adaptation". The global adaptation term constrains the local intensity adaptation term, which is a fine-tuning step. The local adaption term (σ_l(x, y)) is defined as

$$\sigma_l(x,y) = \sigma_g.\frac{L_{in}(x,y)}{1+\omega_s.S_l(x,y)} \tag{3.9}$$

where $S_l(x,y)$ is obtained by calculating the standard deviation of the luminance channel inside a limited window (for instance, 21 X 21) of the structure-pathway L_{in}. The local adaptation factor ($\omega_l(x, y)$), which works well to brighten the dark parts and preserve the bright regions, is similar to the global adaptation factor in that it depends on the local light level and the standard deviation in the local regions. Keep in mind that, L_{in}(x, y) is used as the luminance channel's intensity, directly rather than calculating the local mean because L_{in}(x, y) comes from the foundation layer, which reflects the image's structure and is essentially noise-free.

The updated NR equation (3.7) integrates the global and local adaption elements, and the weights of the terms are spatially adjusted based on the local luminance, which is specified as:

$$\omega_g(x,y) = L_{in}(x,y)^k \tag{3.10}$$

$$\omega_l(x,y) = 1 - \omega_g(x,y) \tag{3.11}$$

where,k is a variable that regulates how much each local and global adaptation term contributes. In the section on experiments, the impact of k on the outcomes will be examined. In the equation 3.7, n regulates the slope of S-shape curves and aids in the improvement of contrast. In this study, the global contrast enhancement factor is calculated as a related measure to the global adaption term (g), which is denoted by

$$n = exp(\sigma_g) \tag{3.12}$$

where n will be between [1, 2.7] approximately because σ_g has a [0, 1] range. As seen in Figure 3.4 for the curves with varying n, it is a reasonable range

for global contrast scaling. There is an implied limitation that substantial scaling of the global contrast should be avoided for dark scenes as that could result in the loss of details in the dark regions given that the estimated global adaption term (σ_{g}) represents the light level of the input image.

Additionally, dynamic range adjustment may lessen some local contrast of some places. Consequently, we create a new local contrast enhancement operator that is optional and supplementary. It is meant for sharpening the image details using a Gaussian (DoG) filter, which is expressed as

$$L_{out}(x,y) = (1+\omega_{dog}).L_{out}(x,y) - \omega_{dog}.(L_{out} * G)(x,y) \tag{3.13}$$

$$G(x,y) = \frac{1}{2\pi\delta_c^2} exp(\frac{-(x^2+y^2}{2\delta_c^2}) \tag{3.14}$$

For this investigation, we chose c = 21 for the night photographs (about 400 x 300 pixels). Additionally, for all trials in this work, we fixed ωdog = 0.5.

The increased luminance maps are then subjected to a standard post-processing step that involves clipping the pixels that are outside of the range [0, 1] and normalising. The improved luminance map could be used to convert from HSV to RGB colour spaces to provide the desired outcome. However, it is discovered that for some photographs with extremely intense light sources, immediately acquiring the output RGB image converted from HSV (HSV RGB) may result in an over-saturated appearance. Because of this, a different effective technique is proposed for minimising the color shift when recombining the luminance values into a colour image, which incorporates an exponent s to regulate the colour saturation. The final colour image that has been processed is obtained by

$$O_{base}^{c}(x,y) = L_{out}(x,y)\left(\frac{I_{base}^{c}(x,y)}{L_{in}(x,y)}\right)^{s} \tag{3.15}$$

where s is a parameter used to adjust colour shift, and in this work, we used s = 0.6. As a result, the structure-pathway processes the increased base layer. Several instances of luminance modification outcomes in the structure pathway are shown in Figure 3.4. Detail – preserved noise suppression are shown in detail - pathway.

Figure 3.4: Examples of luminance adjustment in the structure pathway.

3.3 Detail-preserved noise suppression in detail pathway

Images taken in low light frequently have severe noise interference, which is unavoidable, especially when using some poor-quality cameras. Noise suppression is a vital step to increase the visibility of the enhanced nighttime landscapes. In reality, a number of denoising techniques have been developed and demonstrated to function well on high resolution daylight photos, including Non-local Mean [64] and BM3D [65]. There are also other enhancing techniques for low-light photos that use particular denoising operators as post-processing to get rid of noises [24]. Denoising, however, can reduce noise from some low-resolution photos while also obstructing the details.

In order to reduce noise and maintain details of an input image, it is better to employ noise suppression rather than noise removal. Additionally, noise suppression is incorporated in the detail-pathway, which might somewhat miti-

gate the disruption from low-frequency information. High-frequency details and noises are divided into the detail-pathway using the structure texture decomposition in (1)–(4). As a result, the assumption that the noise level is constant over the entire scene is used in order to estimate the local noises. The local energy of the detail layer can then be used to estimate the local noise level with reasonable accuracy.

Since the regions with the lowest local energy are typically smooth regions (like the sky), which mostly include sounds, it is assumed that these regions indicate the noise level of the image. The combination of the regional specifics and noises should be present in other places with higher energy, in contrast.

In order to calculate the weights of detail preservation (μ^c (x, y)) with the local energy of detail layer, we use the formula:

$$\mu^c(x, y) = (|I^c_{detail}| * G)(x, y) \tag{3.16}$$

where G(x, y) denotes a Gaussian filter defined in the Equation 3.14, and $*$ means the convolution operator. A low weight of detail preservation, as described in (3.16), means that the point (x, y) would be in a smooth zone that lacks detail and should be suppressed. A extremely high μ^c (x, y), on the other hand, suggests that the point (x, y) may be located in the areas that contain details and should be maintained. As a result, the detail-pathway may achieve our detail-preserved noise suppression by

$$O^c_{detail}(x, y) = O^c_{detail}(x, y).\mu^c(x, y) \tag{3.17}$$

Examples of detail-preserved noise suppression in the detail-pathway are shown in Fig 3.6.

It is evident from Fig. 3.6(b) that the detail layer decomposed from a nighttime image typically has substantial noises, particularly in the smooth areas, like the sky. The local energy indicated in (16) can be used to accurately estimate the weights of detail preservation, as seen in Fig. 3.6. (c). Fig. 3.6(d) displays the processed detail maps with detail-preserving noise

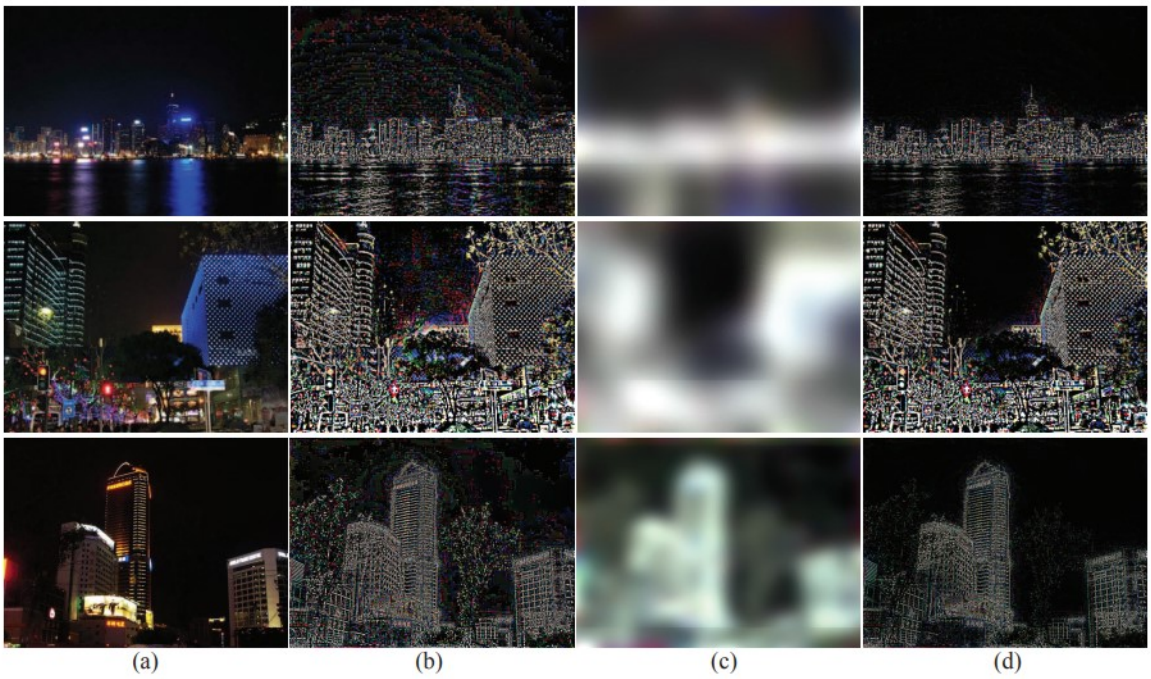

Figure 3.5: The detail preserved noise suppression in the detail layer. a) nighttime images; b)the detail maps (only the positive values); c) the weights of detail preservation based on local noise estimation; d)the detail maps with detail preserved noise suppression.

suppression, where the smooth regions' sounds are successfully suppressed and the structure details (such as the buildings) are well retained.

3.4 Reconstruction of the Final Image

The luminance enhanced map from the structure-pathway and the detail map with noise suppression from the detail-pathway are obtained once the input picture has been processed through both the structure-pathway and detail-pathway. Finally, using the processed base layer and detail layer, the final result is received by using the formula,

$$O^c(x,y) = O^c_{base}(x,y) + \omega_d . O^c_{detail}(x,y) \tag{3.18}$$

where ω_{d} is utilised to balance the detail enhancement and noise suppression. The final enhanced result map of a low-light or nighttime image will then be obtained by the post-processing steps of pixel clipping and normalising.

3.5 Denoising using Anisotropic Diffusion Filter

The methodology is based on the idea that the estimation of the pixel intensity increment or decrement in terms of the directional derivatives with respect to nearby pixels inside an open subset can be used to anticipate the value of the candidate pixel's intensity in the near future[56]. In relation to the pixel in the middle of a 3 X 3 window, the open subset consists of four neighbourhood pixels along the north, south, east, and west axes. Einstein's stochastic defence of Brownian motion led to the creation of the prediction equation, a revolutionary mathematical model. Four nearby pixels, a weighting function, a control parameter, a candidate pixel, and a mathematical model make up the model. An algorithm is produced by translating the mathematical model. Einstein's stochastic argument for Brownian motion served as the basis for the development of the prediction equation, a revolutionary mathematical model. A candidate pixel, four nearby pixels, a weighting function, and a control parameter make up the mathematical model. The algorithm is converted from the mathematical model. The candidate pixel's directional derivatives along its north, south, east, and west axes are computed for the algorithm's numerical computation, and a median estimate of these derivatives is obtained. The median estimate of the directional derivatives is multiplied by a value to update the candidate pixel intensity value. For each pixel in the image, this process is repeated. Until the desired signal to noise ratio performance is attained, the entire method is iterated n times[56].

With regard to an image pixel (${I^n}_{i,j}$), or the centre pixel, and its four neighbours along the north(${I^n}_{i-1,j}$), south(${I^n}_{i+1,j}$), east(${I^n}_{i,j+1}$), and west(${I^n}_{i,j-1}$)directions, the following steps are included in the algorithm given below:

1. Determine the differences in pixel intensities between each surrounding pixel along each direction and the central pixel to obtain the four directional derivatives of the centre pixel along the four directions of north, south, east, and west. The initial row, last row, first column, and last column of an image can all be processed using pixel padding.
2. Decide which of the four directional derivatives from step 1 has the median value.

3.Find the value of the weighting function using the analytical formula given in the below equation, Using the median value the directional derivatives of step 2,

$$g(Med[\Delta_{\mathrm{k}}I] = exp(-(Med[\Delta_{\mathrm{k}}I]/K])) \tag{3.19}$$

4. Choose a suitable control parameter (λ) value between 0 and 1, which provides the best performance for the supplied input image.
5. Locate a scalar value that is the sum of the values from steps 2, 3, and 4. Add the value from step 5 to the pixel intensity of the centre pixel (${I^n}_{i,j}$) to obtain the revised pixel intensity value (${I^{n+1}}_{i,j}$)
7.The same process needs to be expanded to three image planes when dealing with colour photos.

Chapter 4

Experimental Results and Discussion

In this section, we will demonstrate the performance of the proposed method for two visual enhancement related tasks: (1) LDR image enhancement and (2) HDR scene tone mapping.

4.1 Parameter Setting

We empirically adjusted the free parameters in our model to the following values: $\omega_s = 5.0$ in (3.8 and 3.9), k = 0.2 in (10), and $\omega_d = 5.0$ in order to assess the performance of the suggested strategy (3.18). First of all, since S_g is typically much smaller than 1.0, it has a minimal impact on the majority of scenes. Particularly, when dealing with situations with various luminance distributions, the contrast-aware estimation of the adaptation factors in (3.8)–(3.9) improves the robustness. The luminance of the output scene will be improved for some scenes with larger value of S_g, though, as increasing S_g will result in a decrease in the value of the global term. $\omega_s = 5.0$.

4.2 LDR image enhancement

In this study, the technique for the LDR image enhancement challenge is assessed using the PKUnight dataset. PKUnight refers to the subset of the PKU-EAQA dataset that includes 100 nighttime photographs [59], the majority of which are 400 X 300 pixels in size. You can obtain this dataset by visiting https://www.pkuml.org/resources/pku-eaqa.html.

The performance is furthur evaluated with the quantitative metrics called Tone Mapped Image Quality Index, also called TMQI. TMQI is used to eval-

uate the perform the LDR enhancement methods although it is designed for evaluating tone mapping methods.

The output obtained corresponding to the given input image is given the figure 4.1.

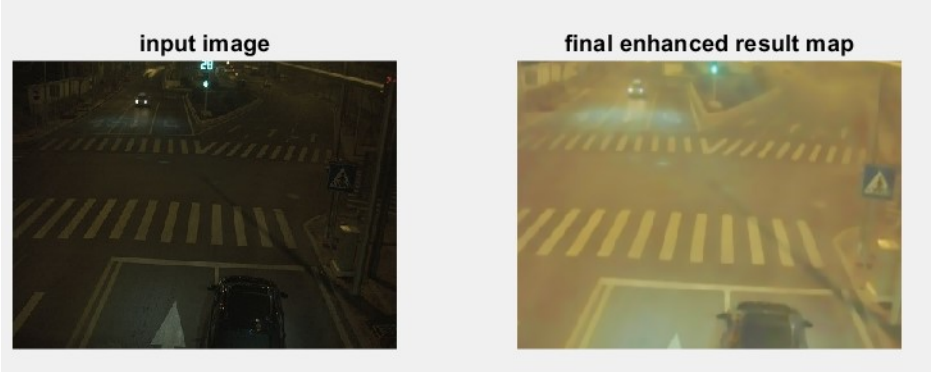

Figure 4.1: The input image and its corresponding output image.

Note that a higher value of TMQI score represent better image quality. In terms of TMQI, the proposed method also obtains acceptable performance. In particular, the method obtains the best TMQI with the remarkably highest value on PKUnight dataset.

Images	Without PM model			With PM model		
	low	high	average	low	high	average
N-[1-100]-0	0.537349	0.809105	0.708172	0.550330	0.834074	0.743832
N-[1-100]-1	0.665998	0.901645	0.796951	0.654495	0.969100	0.868488
N-[1-100]-2	0.552567	0.898863	0.729353	0.644089	0.933511	0.770076
N-[1-100]-3	0.408134	0.903385	0.749540	0.641650	0.985294	0.887087
N-[1-100]-4	0.673351	0.900509	0.759379	0.631890	0.960573	0.806162
N-[1-100]-5	0.299921	0.822377	0.669526	0.513982	0.863332	0.750932

Table 4.1: Performance of the proposed image enhancement framework on the PKunight dataset with quantitative evaluation.

The PKUnight datset consists of 100 images. Each image is captured under six different illumination conditions. The performance of the model is evaluated by finding the lowest, highest and average values of TMQI of the images taken under same illumination conditions. Before applying anisotropic diffusion filter, the model shows an average performance of 0.708172 for images ranging from N-001-0 to N-100-0 (taken under nighttime). After applying anisotropic diffusion filter, the performance of the proposed image enhancement framework has increased from 0.708172 to 0.743832.The lowest TMQI value after applying anisotropic diffusion filter has raised from 0.537349 to 0.550330. Similarly, the highest value of TMQI after applying anisotropic diffusion filter has shown a significant increase from 0.809105 to 0.834074. Before applying anisotropic diffusion filter, the model shows an average performance of 0.796951 for images ranging from N-001-1 to N-100-1. After applying anisotropic diffusion filter, the performance of the proposed image enhancement framework has increased from 0.796951 to 0.868488. Similarly, for images ranging from N-001-2 to N-100-2,the model has shown a superior performance in TMQI.Before applying anisotropic diffusion filter (also called Perona Malik model), the model shows an average performance of 0.729353 for images ranging from N-001-2 to N-100-2. After applying anisotropic diffusion filter, the performance of the proposed image enhancement framework has increased from 0.729353 to 0.770076.The lowest TMQI value on applying anisotropic diffusion filter has raised from 0.552567 to 0.644089. Similarly, the highest value of TMQI after applying anisotropic diffusion filter has shown a significant increase from 0.898863 to 0.933511.For images ranging from N-001-3 to N-100-3,the model has shown a superior performance in terms of TMQI. After applying anisotropic diffusion filter, the performance of the proposed image enhancement framework has increased to 0.887087.The lowest TMQI value on applying anisotropic diffusion filter has raised from 0.408134 to .641650. Similarly, the highest value of TMQI after applying anisotropic diffusion filter has shown a significant increase from 0.903385 to 0.985294. Similarly, the proposed model is evaluated for images ranging from N-001-4 to N-100-4 and N-001-5 to N-100-5. The results are given in the table 4.1.

Chapter 5

Conclusion and Future Works

In this work, a biological visual mechanisms inspired image enhancement framework is studied. In particular, the two-pathway processing can efficiently disassemble the wrapped problems of low-quality images into multiple specific tasks, including luminance brightening, detail enhancing, noise suppressing, etc. In addition, a global to-local strategy is systematically employed for luminance adaptation, contrast enhancement and noise estimation. Extensive experiments on different datasets show that this method can be directly used for nighttime and low-light image enhancement and simply extended for HDR image tone mapping, and provide quite comparable performance in comparison to the recent state-of-the-art methods, but in a quite faster way. As an image enhancement method in poor visibility conditions, this method focuses on improving the visibility of the details especially in dark or low light regions. Brightening the dark regions may sacrifice a little the dynamic range of the whole scene, and hence lead to a little loss of visual naturalness of the processed images. Therefore, as future works, introducing some more flexible visual adaptation mechanisms is expected to further improve the visibility of details and the visual naturalness of the enhanced images.

References

[1] Leonid I.Rudin,Stanley Osher and Emad Fatemi "Nonlinear total variation based noise removal algorithms," Cognitech Inc., 2800, 28th Street, Suite 101, Santa Monica, CA 90405, USA

[2] Jean Franc¸ Ois Aujol, Guy Gilboa, Tony Chan AND Stanley Osher, "Structure-Texture Image Decomposition—Modeling, Algorithms, and Parameter Selection," International Journal of Computer Vision 2006 Springer Science + Business Media, Inc. Manufactured in The Netherlands.

[3] John Immerkær, "Fast Noise Variance Estimation," Computer Vision and Image Understanding Volume 64, Issue 2, September 1996, Pages 300-302.

[4] Jiang, Xuesong Yao, Hongxun Liu, Dilin. (2019). Nighttime image enhancement based on image decomposition. Signal, Image and Video Processing. 13. 10.1007/s11760-018-1345-2.

[5] Laurence Meylan, David Alleysson and Sabine Süsstrunk1, "Model of retinal local adaptation for the tone mapping of color filter array images," Vol. 24, No. 9/September 2007/J. Opt. Soc. Am.

[6] Shawn R. Olsen, Vikas Bhandawat, Rachel I. Wilson, Divisive Normalization in Olfactory Population Codes, Neuron, Volume 66, Issue 2, 2010, Pages 287-299, ISSN 0896-6273.

[7] A. Buades, B. Coll and J. -. Morel, "A non-local algorithm for image denoising", 2005 IEEE Computer Society Conference on Computer Vision and Pattern Recognition (CVPR'05), 2005, pp. 60-65 vol. 2, doi: 10.1109/CVPR.2005.38.

[8] K. Dabov, A. Foi, V. Katkovnik and K. Egiazarian, "Image Denoising by Sparse 3-D Transform-Domain Collaborative Filtering," in IEEE Transactions on Image Processing, vol. 16, no. 8, pp. 2080-2095, Aug. 2007, doi: 10.1109/TIP.2007.901238.

[9] F. Rieke and M. E. Rudd, "The challenges natural images pose for visual adaptation," Neuron, vol. 64, no. 5, pp. 605–616, 2009.

[10] Y. LeCun, Y. Bengio, and G. Hinton, "Deep learning," nature, vol. 521, no. 7553, p. 436, 2015.

[11] H. Kuang, X. Zhang, Y.-J. Li, L. L. H. Chan, and H. Yan, "Nighttime vehicle detection based on bio-inspired image enhancement and weighted score-level feature fusion," IEEE Trans. Intelligent Transportation Systems, vol. 18, no. 4, pp. 927–936, 2017.

[12] S. M. Pizer, E. P. Amburn, J. D. Austin, R. Cromartie, A. Geselowitz, T. Greer, B. ter Haar Romeny, J. B. Zimmerman, and K. Zuiderveld, "Adaptive histogram equalization and its variations," Computer Vision, Graphics, and Image Processing, vol. 39, no. 3, pp. 355–368, 1987.

[13] Y.-T. Kim, "Contrast enhancement using brightness preserving bihistogram equalization," IEEE Trans. Consumer Electronics, vol. 43, no. 1, pp. 1–8, 1997.

[14] E. D. Pisano, S. Zong, B. M. Hemminger, M. DeLuca, R. E. Johnston, K. Muller, M. P. Braeuning, and S. M. Pizer, "Contrast limited adaptive histogram equalization image processing to improve the detection of simulated spiculations in dense mammograms," Journal of Digital Imaging, vol. 11, no. 4, pp. 193–200, 1998.

[15] T. Celik and T. Tjahjadi, "Contextual and variational contrast enhancement," IEEE Trans. Image Processing, vol. 20, no. 12, pp. 3431–3441, 2011.

[16] C. Lee, C. Lee, and C.-S. Kim, "Contrast enhancement based on layered difference representation of 2D histograms," IEEE Trans. Image Processing, vol. 22, no. 12, pp. 5372–5384, 2013.

[17] E. H. Land and J. J. McCann, "Lightness and retinex theory," Journal of the Optical Society of America A: Optics, Image Science Vision, vol. 61, no. 1, pp. 1–11, 1971.

[18] D. J. Jobson, Z.-u. Rahman, and G. A. Woodell, "Properties and performance of a center/surround retinex," IEEE Trans. Image Processing, vol. 6, no. 3, pp. 451–462, 1997.

[19] D. J. Jobson, Z.-u. Rahman, and G. A. Woodell, "A multiscale retinex for bridging the gap between color images and the human observation of scenes," IEEE Trans. Image Processing, vol. 6, no. 7, pp. 965–976, 1997.

[20] S. Wang, J. Zheng, H.-M. Hu, and B. Li, "Naturalness preserved enhancement algorithm for non-uniform illumination images," IEEE Trans. Image Processing, vol. 22, no. 9, pp. 3538–3548, 2013.

[21] X. Fu, D. Zeng, Y. Huang, X.-P. Zhang, and X. Ding, "A weighted variational model for simultaneous reflectance and illumination estimation," in IEEE Conference on Computer Vision and Pattern Recognition, 2016, pp. 2782–2790.

[22] S. Park, S. Yu, B. Moon, S. Ko, and J. Paik, "Low-light image enhancement using variational optimization-based retinex model," IEEE Trans. Consumer Electronics, vol. 63, no. 2, pp. 178–184, 2017.

[23] M. Li, J. Liu, W. Yang, X. Sun, and Z. Guo, "Structure-revealing lowlight image enhancement via robust retinex model," IEEE Trans. Image Processing, vol. 27, no. 6, pp. 2828–2841, 2018.

[24] X. Guo, Y. Li, and H. Ling, "LIME: Low-light image enhancement via illumination map estimation," IEEE Trans. Image Processing, vol. 26, no. 2, pp. 982–993, 2017.

[25] E. Reinhard, W. Heidrich, P. Debevec, S. Pattanaik, G. Ward, and K. Myszkowski, High dynamic range imaging: acquisition, display, and image-based lighting. Morgan Kaufmann, 2010.

[26] L. Meylan and S. Susstrunk, "High dynamic range image rendering with a retinex-based adaptive filter," IEEE Trans. image processing, vol. 15, no. 9, pp. 2820–2830, 2006.

[27] S. Gao, W. Han, Y. Ren, and Y. Li, "High dynamic range image rendering with a luminance-chromaticity independent model," in International Conference on Intelligent Science and Big Data Engineering. Springer, 2015, pp. 220–230.

[28] F. Durand and J. Dorsey, "Fast bilateral filtering for the display of highdynamic-range images," in ACM Transactions on Graphics, vol. 21, no. 3. ACM, 2002, pp. 257–266.

[29] R. Mantiuk, K. J. Kim, A. G. Rempel, and W. Heidrich, "HDR-VDP2: a calibrated visual metric for visibility and quality predictions in all luminance conditions," in ACM Transactions on Graphics, vol. 30, no. 4. ACM, 2011, p. 40.

[30] R. Fattal, D. Lischinski, and M. Werman, "Gradient domain high dynamic range compression," in ACM Transactions on Graphics, vol. 21, no. 3. ACM, 2002, pp. 249–256.

[31] J. Kuang, H. Yamaguchi, C. Liu, G. M. Johnson, and M. D. Fairchild, "Evaluating HDR rendering algorithms," ACM Trans. Applied Perception, vol. 4, no. 2, p. 9, 2007.

[32] G. Eilertsen, R. K. Mantiuk, and J. Unger, "A comparative review of tone-mapping algorithms for high dynamic range video," in Computer Graphics Forum, vol. 36, no. 2. Wiley Online Library, 2017, pp. 565–592.

[33] R. Mukherjee, K. Debattista, T. Bashford-Rogers, M. Bessa, and A. Chalmers, "Uniform color space based high dynamic range video compression," IEEE Trans. Circuits and Systems for Video Technology, p. in press, 2018.

[34] T. Mertens, J. Kautz, and F. Van Reeth, "Exposure fusion: A simple and practical alternative to high dynamic range photography," Computer Graphics Forum, vol. 28, no. 1, pp. 161–171, 2009.

[35] X. Fu, D. Zeng, Y. Huang, Y. Liao, X. Ding, and J. Paisley, "A fusion-based enhancing method for weakly illuminated images," Signal Processing, vol. 129, pp. 82–96, 2016.

[36] Z. Ying, G. Li, and W. Gao, "A bio-inspired multi-exposure fusion framework for low-light image enhancement," arXiv preprint arXiv:1711.00591, 2017.

[37] Z. Li and J. Zheng, "Single image brightening via exposure fusion," in IEEE International Conference on Acoustics, Speech and Signal Processing. IEEE, 2016, pp. 1756–1760.

[38] Z. Li, Z. Wei, C. Wen, and J. Zheng, "Detail-enhanced multi-scale exposure fusion," IEEE Trans. Image Processing, vol. 26, no. 3, pp. 1243–1252, 2017.

[39] S. Wu, J. Xu, Y.-W. Tai, and C.-K. Tang, "Deep high dynamic range imaging with large foreground motions," in European Conference on Computer Vision. Springer, 2018, pp. 120–135.

[40] N. K. Kalantari and R. Ramamoorthi, "Deep high dynamic range imaging of dynamic scenes," ACM Transactions on Graphics, vol. 36, no. 4, p. 144, 2017.

[41] G. Eilertsen, J. Kronander, G. Denes, R. K. Mantiuk, and J. Unger, "HDR image reconstruction from a single exposure using deep CNNs," ACM Transactions on Graphics, vol. 36, no. 6, p. 178, 2017.

[42] Y. Endo, Y. Kanamori, and J. Mitani, "Deep reverse tone mapping," ACM Transactions on Graphics, vol. 36, no. 6, 2017.

[43] K. G. Lore, A. Akintayo, and S. Sarkar, "LLNet: A deep autoencoder approach to natural low-light image enhancement," Pattern Recognition, vol. 61, pp. 650–662, 2017.

[44] L. Shen, Z. Yue, F. Feng, Q. Chen, S. Liu, and J. Ma, "MSR-net: Low-light image enhancement using deep convolutional network," arXiv preprint arXiv:1711.02488, 2017.

[45] M. Carandini and D. J. Heeger, "Normalization as a canonical neural computation," Nature Reviews Neuroscience, vol. 13, no. 1, pp. 51–62, 2012.

[46] T. Gollisch and M. Meister, "Eye smarter than scientists believed: neural computations in circuits of the retina," Neuron, vol. 65, no. 2, pp. 150– 164, 2010.

[47] E. P. Simoncelli and B. A. Olshausen, "Natural image statistics and neural representation," Annual Review of Neuroscience, vol. 24, no. 1, pp. 1193–1216, 2001.

[48] K. Naka and W. Rushton, "S-potentials from colour units in the retina of fish (cyprinidae)," The Journal of Physiology, vol. 185, no. 3, pp. 536–555, 1966.

[49] Z. Xie and T. G. Stockham, "Toward the unification of three visual laws and two visual models in brightness perception," IEEE Trans. Systems, Man, and Cybernetics, vol. 19, no. 2, pp. 379–387, 1989.

[50] X. Pu, K. Yang, and Y. Li, "A retinal adaptation model for HDR image compression," in CCF Chinese Conference on Computer Vision. Springer, 2017, pp. 37–47.

[51] P. H. Schiller, "Parallel information processing channels created in the retina," Proceedings of the National Academy of Sciences, p. 201011782, 2010.

[52] E. Kaplan, "The M, P, and K pathways of the primate visual system," The Visual Neurosciences, vol. 1, pp. 481–493, 2004.

[53] L. Meylan, D. Alleysson, and S. Susstrunk, "Model of retinal local ¨ adaptation for the tone mapping of color filter array images," Journal of the Optical Society of America A: Optics, Image Science Vision, vol. 24, no. 9, pp. 2807–2816, 2007.

[54] K.-F. Yang, H. Li, H. Kuang, C.-Y. Li, and Y.-J. Li, "An adaptive method for image dynamic range adjustment," IEEE Trans. Circuits and Systems for Video Technology, p. in press, 2018.

[55] X.-S. Zhang and Y.-J. Li, "A retina inspired model for high dynamic range image rendering," in International Conference on Brain Inspired Cognitive Systems. Springer, 2016, pp. 68–79.

[56] Resmi R. Nair , Ebenezer David and Sivakumar Rajagopal, "A robust anisotropic diffusion filter with low arithmetic complexity for images", EURASIP Journal on Image and Video Processing (2019) 2019:48 https://doi.org/10.1186/s13640-019-0444-5

[57] L. I. Rudin, S. Osher, and E. Fatemi, "Nonlinear total variation based noise removal algorithms," Physica D: Nonlinear Phenomena, vol. 60, no. 1-4, pp. 259–268, 1992.

[58] Y. Li, F. Guo, R. T. Tan, and M. S. Brown, "A contrast enhancement framework with JPEG artifacts suppression," in European Conference on Computer Vision. Springer, 2014, pp. 174–188.

[59] C. Li and Z. He, "Effects of patterned backgrounds on responses of lateral geniculate neurons in cat," Experimental brain research, vol. 67, no. 1, pp. 16–26, 1987.

[60] J. Immerkaer, "Fast noise variance estimation," Computer Vision and Image Understanding, vol. 64, no. 2, pp. 300–302, 1996.

[61] X. Jiang, H. Yao, and D. Liu, "Nighttime image enhancement based on image decomposition," Signal, Image and Video Processing, pp. 1–9, 2018.

[62] A. R. Smith, "Color gamut transform pairs," ACM Siggraph Computer Graphics, vol. 12, no. 3, pp. 12–19, 1978.

[63] S. R. Olsen, V. Bhandawat, and R. I. Wilson, "Divisive normalization in olfactory population codes," Neuron, vol. 66, no. 2, pp. 287–299, 2010.

[64] A. Buades, B. Coll, and J.-M. Morel, "A non-local algorithm for image denoising," in IEEE Conference on Computer Vision and Pattern Recognition, vol. 2. IEEE, 2005, pp. 60–65.

[65] K. Dabov, A. Foi, V. Katkovnik, and K. Egiazarian, "Image denoising by sparse 3-D transform-domain collaborative filtering," IEEE Trans. Image Processing, vol. 16, no. 8, pp. 2080–2095, 2007.

[66] H. Yue, J. Yang, X. Sun, F. Wu, and C. Hou, "Contrast enhancement based on intrinsic image decomposition," IEEE Trans. Image Processing, vol. 26, no. 8, pp. 3981–3994, 2017.

[67] Z. Chen, T. Jiang, and Y. Tian, "Quality assessment for comparing image enhancement algorithms," in IEEE Conference on Computer Vision and Pattern Recognition, 2014, pp. 3003–3010.

[68] A. R. Rivera, B. Ryu, and O. Chae, "Content-aware dark image enhancement through channel division," IEEE Trans. Image Processing, vol. 21, no. 9, pp. 3967–3980, 2012.

[69] L. Zhang, L. Zhang, and A. C. Bovik, "A feature-enriched completely blind image quality evaluator," IEEE Trans. Image Processing, vol. 24, no. 8, pp. 2579–2591, 2015.